ISSN 1063-7729, Astronomy Reports, 2007, Vol. 51, No. 7, pp. 549–562. © Pleiades Publishing, Ltd., 2007.
Original Russian Text © V.F. Suleimanov, G.V. Lipunova, N.I. Shakura, 2007, published in Astronomicheskiĭ Zhurnal, 2007, Vol. 84, No. 7, pp. 612–626.

The Thickness of Accretion α-Disks: Theory and Observations

V. F. Suleimanov[1,2], G. V. Lipunova[3], and N. I. Shakura[3]

[1] *Kazan State University, ul. Lenina 18, Kazan, 420008 Tatarstan, Russia*

[2] *Institute for Astronomy and Astrophysics (IAAT) of the Eberhard-Karls- University of Tubingen, Sand 1, D-72076 Tubingen, Germany*

[3] *Sternberg Astronomical Institute, Universitetskiĭ pr. 13, Moscow, 119899 Russia*

Received December 17, 2006; in final form, December 27, 2006

Abstract—Observations of X-ray binaries indicate substantial half-thicknesses for the accretion disks in these systems (up to $h/R \approx 0.25$, where h is the disk half-thickness and R its radius), while standard α accretion disks predict appreciably smaller half-thicknesses. We study the theoretical vertical structure of such disks using two independent numerical methods, and show that their maximum half-thicknesses in the subcritical regime cannot exceed $h/R \approx 0.1$. We consider various reasons for the apparent increase in the disk thickness, the most probable of which is the presence of matter above the disk in the form of a hot corona that scatters hard radiation from the central source and inner parts of the disk. As a result, the observed thickness of the disk and the illumination of its outer parts effectively increase. This mechanism can also explain both the optical-to-X-ray flux ratio in these systems and the observed parameters of eclipsing X-ray binaries.

PACS numbers : 97.10.Gz, 97.80.Jp
DOI: 10.1134/S1063772907070049

1. INTRODUCTION

It is currently believed that disk accretion provides the source of energy radiated by various astrophysical objects. In disk accretion, matter rotates about a gravitating center along essentially circular orbits approximately in a single plane. The disk radiates due to viscous friction, and the matter drifts towards the center. Present models for accretion disks are based on (or are inevitably compared with) the theory developed by Shakura and Syunyaev [1] in 1973, which has since acquired the status of a standard model of accretion in binaries and galactic nuclei (see, for example, [2, 3]). Models based on Shakura–Sunyaev accretion-disk theory can explain both the overall energy released by the objects (X-ray binaries, cataclysmic variables, active galactic nuclei) and, in many cases, the spectral energy distributions (SEDs) and dynamics of non-stationary events occurring in them. In particular, dwarf and X-ray nova outbursts are very consistent with the α-disk model when the partial ionization of hydrogen in their outer regions is taken into account [4–7]. The light curves of X-ray novae are in good agreement with the non-stationary α-disk model [8–9] at the stage of viscous evolution, when the disk material is totally ionized. In general, the dynamics of disk accretion in real astrophysical objects is adequately described under the assumptions of the thin α-disk model (see, however, the discussion in Section 6).

The geometrical thicknesses of real accretion disks in close binaries have been estimated using various indirect methods. There is some evidence in a number of cases that the relative half-thickness of the disk is appreciable, exceeding the thickness of a standard thin Shakura–Syunyaev disk by the factor of 1.5–3. Thus, there is a discrepancy between the disk thicknesses derived from the dynamics of accretion disks and from their geometry, which is used in models of radiation from binaries with accretion disks.

Here, we model the vertical structure of the disk and use two independent methods to obtain the radial dependence for the attainable disk thickness of a standard accretion disk. We also discuss possible reasons why a thin accretion disk may manifest itself like a more extended object.

In general, the vertical structure of accretion disks (both stationary and non-stationary) is described by a system of four ordinary differential equations, whose exact solution for specified boundary conditions can be found using numerical techniques. Introducing the equation for the angular momentum integrated over the vertical coordinate enables us to find the radial structure of a stationary accretion disk. The system of differential equations for the vertical structure of the

disk has been solved in a number of studies (see, for example, [10–16]).

We consider two different approaches to solving this system of equations. In the first approach, we solved the system numerically, taking into account the real opacity, together with the contributions of gas and radiation pressure. We use values from opacity tables for gas with solar chemical composition for the Rosseland mean opacity [17–19].

The second approach, which was proposed and realized in [15], involves searching for similar solutions to the system of vertical structure equations reduced to dimensionless form using the analytical approximation for the opacity coefficient

$$\kappa = \kappa_0 \rho^\zeta / T^\nu. \quad (1)$$

This approximation has two versions, leading to the disk being divided into two zones. The power-law indices ζ and ν depend on the main processes contributing to the opacity. Closer to the disk center, Thomson scattering on free electrons dominates, while photoionization of heavy-element ions and free–free transitions dominates at larger distances. The radiation pressure in these two zones can be neglected.

Close to the disk center, where the radiation pressure dominates in the case of high accretion rates, the matter displays viscous (secular) and thermal instabilities [20–22], while ionization–thermal instability develops at large distances, due to the onset of hydrogen recombination [4]. Thus, in general, the stable zone in the disk is restricted in radius both from the inside and from the outside. For example, for $M \sim 10\ M_\odot$, $\dot{M} \sim 10^{18}$ g/s, $\mu \sim 0.6$, and the turbulence parameter $\alpha \sim 0.1$, the stationary zone of the disk is situated between $\sim 9.3 \times 10^7$ cm and $\sim 6.5 \times 10^{10}$ cm. However, taking into account the illumination of the outer parts of the disk by hard radiation from its central regions, this zone may be extended to 10^{11} [23]. The presented results are valid only in the stationary zones of accretion disks, where the gas pressure dominates and hydrogen is totally ionized.

In the following Section, the equations for the vertical structure of a standard α disk are written out. In Section 3, we describe the applied numerical solution technique. Analytical radial dependences are derived in Section 4, based on the method used to solve for the vertical structure [15]. Section 5 compares the radial dependences constructed based on the different methods used to solve for the vertical structure. In the concluding section, we discuss possible reasons for the discrepancy between the theoretically predicted and observed thicknesses of disks.

2. BASIC EQUATIONS

Let us write the basic equations for stationary disk accretion [1, 24]. We omit relativistic corrections, which take into account general-relativistic effects connected with accretion onto black holes, since we will study regions far from the center. We will consider geometrically thin, optically thick accretion α disks without advection and mass loss from the surface. This means, in particular, that the angular velocity of the disk rotation at each radius R is equal to the Kepler velocity $\omega = \sqrt{GM/R^3}$. The luminosity of such a disk does not exceed the Eddington limit. The parameters specifying the disk structure are the mass of the gravitating center M, the inner radius of the accretion disk $R_{\rm in}$, the accretion rate $\dot{M}$, and the parameter α, which characterizes the viscosity of the disk material. Thus, we have the following equations for an axially symmetric disk in cylindrical coordinates.

The continuity equation

$$2\pi R v_r \int_{-h}^{h} \rho \mathrm{d}z = \dot{M}, \quad (2)$$

where ρ is the density, v_r the radial component of the velocity of the matter, and h the half-thickness of the disk.

The angular-momentum conservation equation

$$2\pi \int_{-h}^{h} w_{r\varphi} \mathrm{d}z = \dot{M}\omega f(R), \quad (3)$$

where $w_{r\varphi}$ is the tangent component of the viscous-stress tensor and $f(R)$ a function containing information on the boundary conditions of the viscous-stress tensor. For a non-relativistic, stationary semi-infinite disk without an outer boundary, $f(R) = 1 - \sqrt{R_{\rm in}/R}$, which corresponds to the condition that the viscous stress is zero at the inner boundary of the disk. Away from the central object, $f(R) \cong 1$.

The condition of hydrostatic equilibrium in the z coordinate

$$\frac{1}{\rho}\frac{\mathrm{d}P}{\mathrm{d}z} = -\omega^2 z, \quad (4)$$

where P is the total pressure in the disk, equal to the sum of the radiation pressure $P_{\rm rad}$ and gas pressure $P_{\rm gas}$, which is specified by the equation of state for an ideal gas,

$$P_{\rm gas} = \frac{\rho \mathcal{R} T}{\mu}, \quad (5)$$

μ is the mean molecular weight of the disk material, and T is the temperature. The component of the viscosity tensor at each point of the disk $w_{r\varphi}$ is expressed

in terms of the total pressure at this point using the parameter α [24]:

$$w_{r\varphi} = \alpha P. \quad (6)$$

We assume that the energy in the disk is transferred in the z direction by radiation. In the case of the Cramers opacity, convection does not develop [25]. We can write the frequency-integrated moments of the stationary equation of radiative transfer: the zero moment,

$$\frac{1}{\rho}\frac{\mathrm{d}Q}{\mathrm{d}z} = 4\pi\kappa_\mathrm{a}(B_T - J), \quad (7)$$

and the first moment in the diffusion approximation,

$$\frac{1}{3\rho}\frac{\mathrm{d}\varepsilon_\mathrm{rad}}{\mathrm{d}z} = -\kappa_\mathrm{r}\frac{Q}{c}. \quad (8)$$

The rate of energy generation is specified by the expression

$$\frac{\mathrm{d}Q}{\mathrm{d}z} = \frac{3}{2}\omega w_{r\varphi}. \quad (9)$$

Here, κ_a is the frequency-averaged true opacity coefficient, which is equal to the Planck mean opacity coefficient if the spectrum of the mean intensity at any point equals the Planck function, κ_r is the Rosseland mean absorption coefficient, Q the radiative energy flux, $B_T = \sigma_\mathrm{SB}T^4/\pi$ the Planck function integrated over frequency, and J the mean intensity of the radiation integrated over frequency, which is related to the radiated energy density

$$\varepsilon_\mathrm{rad} = \frac{4\pi J}{c}. \quad (10)$$

In the case of thermodynamic equilibrium, there exists a simple relation between the radiation energy density and the radiation pressure:

$$P_{rad} = \frac{\varepsilon_\mathrm{rad}}{3}, \quad (11)$$

which we will use below. The other notation is standard.

We will characterize the accretion disk model using the following physical quantities as functions of the radial distance in the disk: the density and temperature in the plane of symmetry of the disk for $z = 0$ ρ_c and T_c, the half-thickness of the disk $h = z(\tau_\mathrm{r} = 2/3)$, where τ_r is the Rosseland optical depth of the disk, and the surface density

$$\Sigma = \int_{-h}^{h} \rho \mathrm{d}z.$$

These quantities must be found from (2)–(9) with the corresponding boundary conditions. The following section describes the solution method used.

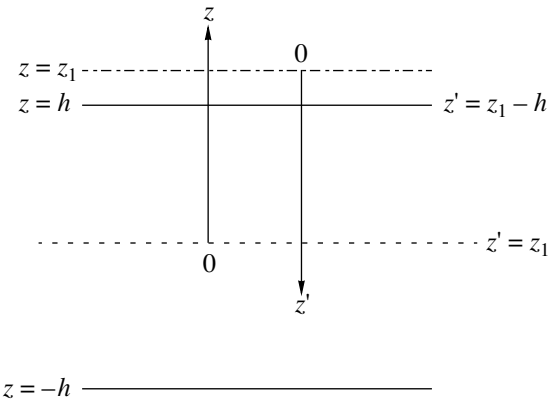

Fig. 1. The coordinate frame in the disk. The dashed line corresponds to the plane of symmetry of the disk, and the solid lines to the surface where $\tau_\mathrm{r} = 2/3$. The dot–dashed line indicates the upper surface of the disk, where $\tau_\mathrm{r} = 0$.

Note that averaging the physical quantities over z makes it possible to reduce the relations used to algebraic equations. If the opacity is taken in the form (1), we obtain solutions analogous to those of [1].

3. A NUMERICAL SOLUTION FOR THE VERTICAL STRUCTURE EQUATIONS

At each radial distance in the disk, its vertical structure can be determined from the solution of the differential equations (4), (8), and (9) with corresponding boundary conditions. We found the temperature using using Eq. (7) for each depth, neglecting the $\mathrm{d}Q/\mathrm{d}z$ term; i.e., the temperature was determined from the thermodynamical relation

$$B_T = J = \frac{\sigma_\mathrm{SB}T^4}{\pi} = \frac{3cP_\mathrm{rad}}{4\pi}.$$

As was shown in [11], including the $\mathrm{d}Q/\mathrm{d}z$ term in (7) (physically, this means that thermal energy is generated at all depths in the disk) for effectively optically thick disks results in the formation of a corona above the disk; however, this affects the temperature of inner optically thick disk layers only insignificantly.

For convenience, (4), (8), and (9) were rewritten in the form

$$\frac{1}{\rho}\frac{\mathrm{d}P}{\mathrm{d}z'} = (z_1 - z')\omega^2, \quad (12)$$

$$\frac{\mathrm{d}Q}{\mathrm{d}z'} = -\frac{3}{2}\alpha P\omega, \quad (13)$$

$$\frac{\mathrm{d}P_\mathrm{rad}}{\mathrm{d}z'} = \frac{\rho\kappa_\mathrm{r}Q}{c}. \quad (14)$$

We introduce here the new variable $z' = z_1 - z$ (Fig. 1), where z_1 is a parameter formally corresponding to the disk half-thickness for $\tau_r = 0$ (in fact, it corresponds to the small optical depth $\tau_r \approx 10^{-5}$–10^{-6} from which the calculations start).

Integrating (9) and taking into account (3), we obtain

$$Q_0 = \frac{3}{8\pi}\omega^2 \dot{M} f(R). \quad (15)$$

Here, $Q_0 = \sigma_{SB} T_{eff}^4$ is the energy flux radiated from the disk surface at a given radius. This expression is independent of details of the disk structure in the z direction, and can be used as a boundary condition at the disk surface.

We adopt the following boundary conditions at the surface ($z' = 0$):

$$Q(0) = Q_0, \qquad \rho(0) = 0,$$
$$P(0) = P_{rad}(0) = \frac{2}{3}\frac{Q_0}{c}.$$

The boundary condition in the plane of symmetry of the disk is the requirement that the radiation flux be zero:

$$Q(z' = z_1) = 0.$$

Thus, we have four boundary conditions for three unknown functions of the independent variable z'. With the given boundary conditions, (12)–(14) can be solved using the method of prediction and correction, moving deeper from the surface for a specified disk half-thickness z_1. z_1 is not known in advance. Of all solutions of (12)–(14), we must choose the one for which z_1 satisfies the boundary condition in the plane of symmetry of the disk. In our case, z_1 was determined by dividing the interval into halves until the condition $Q(z_1) < 0.01\ Q_0$ was fulfilled. In the course of obtaining the solution, the opacity at each depth was determined iteratively until a relative accuracy of 1% was achieved. The current value for κ_r was found from the current T_c and P_{gas} values from the opacity tables [17, 18], which we supplemented towards high temperatures with [19]. Solar chemical composition was assumed [26].

Next, the disk parameters were determined at each radial distance: the half-thickness h, equal to the distance between the disk plane of symmetry and the level with optical depth $\tau_r = 2/3$, and the surface density $\Sigma = 2\int_{z_1-h}^{z_1} \rho dz'$. The radial density $\sigma(z')$ is specified by the fourth differential equation:

$$\frac{d\sigma}{dz'} = \rho. \quad (16)$$

4. RADIAL STRUCTURE OF THE DISK: ANALYTICAL DEPENDENCES

Calculating the vertical structure of the disk using the approach suggested in [15] yields analytical expressions for the radial dependences of the disk parameters. In [15], the opacity coefficient κ_r was taken in the analytical form (1), where the indices ζ and ν depend on the type of opacity in the disk. In zone B, where scattering on free electrons dominates, $\zeta = \nu = 0$; in zone C, where most absorption is due to free–free and bound–free transitions, formula (1) assumes the form of the Cramers formula with $\zeta = 1$ and $\nu = -7/2$. It was also assumed that the radiation pressure in the disk can be neglected. A comparison between the results of the two calculations of the vertical structure showed that, in zone B, this assumption appreciably restricts the accuracy of the solution when $P_{rad} \gtrsim (0.2\text{–}0.3)P_{gas}$.

The method presented in [15] considers a system of equations for the dimensionless functions P/P_c, z/h, Q/Q_o, and T/T_c. The independent variable in the equations used in [15] is the column density measured from the plane of symmetry of the disk and normalized to $\Sigma/2$. The system (12)–(16) contains four dimensionless quantities comprising various combinations of the physical parameters of the disk and the radius R: Π_1, Π_2, Π_3, and Π_4 (see also [27]). The method of [15] also enables calculation of the vertical structure of a non-stationary disk; models applied to X-ray novae were constructed in [8].

Eight boundary conditions are imposed when finding the solution (four functions and four unknown parameters): four at the disk surface and four in the disk plane of symmetry. These boundary conditions contain the free parameter, which is different in zones B and C, and represents a measure of the optical depth of the disk. The disk surface in the two zones is also specified in different ways. In the zone where absorption dominates the opacity, the disk surface is assumed to correspond to the level where the optical depth calculated from infinity to the disk surface is two-thirds, and the temperature is equal to the effective temperature. In the zone where Thomson scattering dominates, the disk surface is assumed to correspond to the level where the radiation is thermalized and the effective optical depth is $\tau^\dagger \cong 1$. The effective optical depth is taken to be $d\tau^\dagger = \sqrt{\kappa_{ff}(\kappa_T + \kappa_{ff})}\rho dz$. The system of equations in [15] was numerically integrated, and $\Pi_1 - \Pi_4$ tabulated as a function of the free parameter, δ, or τ_0. [1]

Using the values of the dimensionless parameters $\Pi_1 - \Pi_4$ from [15], we can find the disk half-thickness

[1] The refined tables in electronic form are available from the authors or at http://xray.sai.msu.ru/galja/data/PPPP/.

h, surface density Σ, density ρ_c, and temperature T_c in the form of radial dependences that also contain the general parameters of the accretion disk. In the stationary mode of disk accretion, we use relation (15) between the flux from the disk surface Q_0 and the accretion rate.

Let us now normalize the disk parameters to their characteristic values for accretion disks in binary systems with stellar-mass components:

$$M = mM_\odot, \quad \dot{M} = \dot{M}_{17} \times 10^{17}\ \mathrm{g/s}, \qquad (17)$$
$$R = R_7 \times 10^7\ \mathrm{cm\ (zone\ B)\ \ or}$$
$$R = R_{10} \times 10^{10}\ \mathrm{cm\ (zone\ C)}.$$

As the characteristic value for the factor κ_0 from (1) in zone B, we use $\kappa_T^* = 0.335\ \mathrm{cm^2/g}$, obtained via an approximation to the tabulated values in [17, 18] for a medium with mass fractions $X = 0.69$ for hydrogen and $Y = 0.27$ for helium; in zone C, we use $\kappa_0^* = 5 \times 10^{24}\ \mathrm{cm^5\ g^{-2}\ K^{7/2}}$ [3, Sec. 5]. The corresponding molecular mass is $\mu = 0.62$. In a medium with this chemical composition, radiation is primarily absorbed as a result of the photoionization of ions of heavy elements.

Thus, in zone B, where, by definition, scattering on free electrons yields the main contribution to the opacity and the gas pressure exceeds the radiation pressure, solving the system of algebraic equations for $\Pi_1 - \Pi_4$ from [15] and using (15) and (17) yields

$$h/R = 0.0092 m^{-7/20} \dot{M}_{17}^{1/5} \alpha^{-1/10} R_7^{1/20} \qquad (18)$$
$$\times f(R)^{1/5} \left(\frac{\mu}{0.6}\right)^{-2/5} \left(\frac{\kappa_T}{\kappa_T^*}\right)^{1/10} \Pi_h,$$
$$\Sigma = 5.1 \times 10^3 m^{1/5} \dot{M}_{17}^{3/5} \alpha^{-4/5} R_7^{-3/5} \qquad (19)$$
$$\times f(R)^{3/5} \left(\frac{\mu}{0.6}\right)^{4/5} \left(\frac{\kappa_T}{\kappa_T^*}\right)^{-1/5} \Pi_\Sigma\ \mathrm{g/cm^2},$$
$$\rho_c = 2.8 \times 10^{-2} m^{11/20} \dot{M}_{17}^{2/5} \alpha^{-7/10} R_7^{-33/20} \qquad (20)$$
$$\times f(R)^{2/5} \left(\frac{\mu}{0.6}\right)^{6/5} \left(\frac{\kappa_T}{\kappa_T^*}\right)^{-3/10} \Pi_\rho\ \mathrm{g/cm^3},$$
$$T_c = 8.2 \times 10^6 m^{3/10} \dot{M}_{17}^{2/5} \alpha^{-1/5} R_7^{-9/10} \qquad (21)$$
$$\times f(R)^{2/5} \left(\frac{\mu}{0.6}\right)^{1/5} \left(\frac{\kappa_T}{\kappa_T^*}\right)^{1/5} \Pi_T\ \mathrm{K}.$$

The combinations of dimensionless parameters Π_h, Π_Σ, Π_ρ, and Π_T are related to the parameters $\Pi_1 - \Pi_4$ as follows:

$$\Pi_h = \Pi_1^{1/2} \Pi_3^{1/10} \Pi_4^{-1/10}, \quad \Pi_\Sigma = \Pi_3^{4/5} \Pi_4^{1/5}, \quad (22)$$
$$\Pi_\rho = \Pi_1^{-1/2} \Pi_2^{-1} \Pi_3^{7/10} \Pi_4^{3/10}, \quad \Pi_T = \Pi_3^{1/5} \Pi_4^{-1/5}.$$

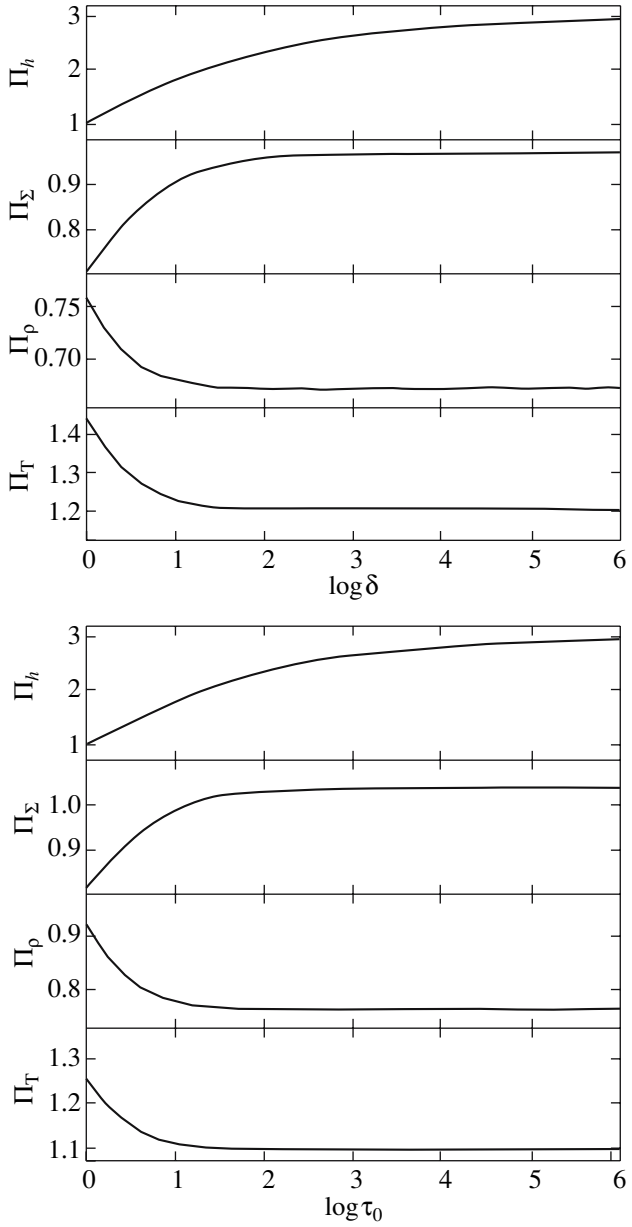

Fig. 2. Dependences of the dimensionless factors on the logarithms of values characterizing the optical depth of the disk, calculated from (22) for the upper graphs and from (31) for the lower graphs (plotted for Table 2a and Table 1a from [15], respectively).

Figure 2 presents their values as functions of the free parameter δ, specified in the form

$$\delta = \frac{\tau}{\tau_T(\tau^\dagger = 1)},$$

where

$$\tau = \kappa_T \frac{\Sigma}{2} \qquad (23)$$

is the optical depth to scattering in the disk and $\tau_T(\tau^\dagger = 1)$ the optical depth to scattering accumu-

lated from infinity to the disk surface at the thermalization depth [15]. The thermalization depth can be defined from the approximate condition (see, for example, [28, 29])

$$\tau^\dagger = -\int\limits_\infty^h \sqrt{\kappa_{\rm ff}\kappa_{\rm T}}\rho {\rm d}z \cong 1.$$

We obtain from the equation for hydrostatic equilibrium in an isothermal approximation the law for the density decrease above the disk, together with the value

$$\delta = \frac{\tau}{\tau_{\rm T}(\tau^\dagger = 1)} = \left[\frac{2^{3/4}}{18}\frac{\rho_{\rm c}\kappa_0}{T_{\rm c}^{7/2}}\kappa_{\rm T}(\rho_{\rm c}h)^2\frac{\Pi_1\Pi_2^3}{\Pi_4^{9/8}}\right]^{8/15},$$

which depends fairly weakly on the disk parameters; with the characteristic values we used for the normalizations in zone B, we can obtain the following estimate, which includes the strongest dependences:

$$\delta \sim 200\left(\frac{\kappa_0}{\kappa_0^*}\right)^{8/15}\Pi_1^{4/15}\frac{R_7^{4/25}\dot{M}_{17}^{8/75}\mu_6^{28/25}}{\alpha^{64/75}}. \quad (24)$$

The optical depth to scattering in zone B calculated from infinity to the thermalization depth, $\tau_{\rm T}(\tau^\dagger = 1)$, exceeds unity, since the scattering is appreciable:

$$\tau_{\rm T}(\tau^\dagger = 1) = \frac{\tau}{\delta} \sim 4\left(\frac{\kappa_{\rm T}}{\kappa_{\rm T}^*}\right)^{76/75}\left(\frac{\kappa_0}{\kappa_0^*}\right)^{-8/15} \quad (25)$$
$$\times\,\Pi_1^{-4/15}\dot{M}_{17}^{37/75}\frac{m^{19/75}}{R_7^{19/25}}.$$

When the accretion rate decreases, zone B shifts in radius towards the disk center, giving way to zone C.

A zone where the radiation pressure dominates appears in the disk near the central object in the case of high accretion rates. The radius where the radiation pressure $aT_{\rm c}^4/3$ and gas pressure $\rho_{\rm c}\mathcal{R}T_{\rm c}/\mu$ become equal in the disk plane of symmetry (the boundary between zones A and B) [1] is roughly estimated as

$$R_{\rm AB} \sim 10^7 m^{1/3}\dot{M}_{17}^{16/21}\alpha^{2/21} \quad (26)$$
$$\times\left(\frac{\mu}{0.6}\right)^{8/21}\left(\frac{\kappa_{\rm T}}{\kappa_{\rm T}^*}\right)^{6/7}\ {\rm cm}.$$

Here, we have adopted the characteristic values for the dimensionless parameters $\Pi_1 - \Pi_4$ and $f(R) = 1$. Expression (26) is an upper estimate, since $f(R) \le 1$.

Further, in zone C, where free–free and bound–free absorption makes the largest contribution to the opacity and the gas pressure is much higher than the radiation pressure, we obtain the expressions

$$h/R = 0.020 m^{-3/8}\dot{M}_{17}^{3/20}\alpha^{-1/10}R_{10}^{1/8} \quad (27)$$
$$\times\, f(R)^{3/20}\left(\frac{\mu}{0.6}\right)^{-3/8}\left(\frac{\kappa_0}{\kappa_0^*}\right)^{1/20}\Pi_h,$$

$$\Sigma = 33 m^{1/4}\dot{M}_{17}^{7/10}\alpha^{-4/5}R_{10}^{-3/4} \quad (28)$$
$$\times\, f(R)^{7/10}\left(\frac{\mu}{0.6}\right)^{3/4}\left(\frac{\kappa_0}{\kappa_0^*}\right)^{-1/10}\Pi_\Sigma\ {\rm g/cm^2},$$

$$\rho_{\rm c} = 8.0\times 10^{-8} m^{5/8}\dot{M}_{17}^{11/20}\alpha^{-7/10}R_{10}^{-15/8} \quad (29)$$
$$\times\, f(R)^{11/20}\left(\frac{\mu}{0.6}\right)^{9/8}\left(\frac{\kappa_0}{\kappa_0^*}\right)^{-3/20}\Pi_\rho\ {\rm g/cm^3},$$

$$T_{\rm c} = 4.0\times 10^4 m^{1/4}\dot{M}_{17}^{3/10}\alpha^{-1/5}R_{10}^{-3/4} \quad (30)$$
$$\times\, f(R)^{3/10}\left(\frac{\mu}{0.6}\right)^{1/4}\left(\frac{\kappa_0}{\kappa_0^*}\right)^{1/10}\Pi_{\rm T}\ {\rm K},$$

where the combinations of the dimensionless parameters are related to $\Pi_1 - \Pi_4$ as follows:

$$\Pi_h = \Pi_1^{19/40}\Pi_2^{-1/20}\Pi_3^{1/10}\Pi_4^{-1/20}, \quad (31)$$
$$\Pi_\Sigma = \Pi_1^{1/20}\Pi_2^{1/10}\Pi_3^{4/5}\Pi_4^{1/10},$$
$$\Pi_\rho = \Pi_1^{-17/40}\Pi_2^{-17/20}\Pi_3^{7/10}\Pi_4^{3/20},$$
$$\Pi_{\rm T} = \Pi_1^{-1/20}\Pi_2^{-1/10}\Pi_3^{1/5}\Pi_4^{-1/10}.$$

Figure 2 presents these quantities as functions of the free parameter

$$\tau_0 = \frac{\kappa_0\rho_{\rm c}}{T_{\rm c}^{7/2}}\frac{\sigma}{2} = 500\frac{\dot{M}_{17}^{1/5}f(R)^{1/5}}{\alpha^{4/5}} \quad (32)$$
$$\times\left(\frac{\mu}{0.6}\right)\left(\frac{\kappa_0}{\kappa_0^*}\right)^{2/5}\frac{\Pi_3^{4/5}\Pi_4^{3/5}}{\Pi_1^{1/5}\Pi_2^{2/5}},$$

which is approximately equal to

$$\tau_0 \sim 300\dot{M}_{17}^{1/5}\alpha^{-4/5}\left(\frac{\kappa_0}{\kappa_0^*}\right)^{2/5}. \quad (33)$$

The total optical depth

$$\tau = \int\limits_0^h \kappa_0\rho^2 T^{-7/2}{\rm d}z \quad (34)$$

was found in [15] in the course of the numerical solution for the vertical structure equations, and depends unambiguously on τ_0. We also present a formula that approximates the tabulated values with an accuracy better than 1% for $\tau_0 > 6$:

$$\tau \approx 1.042\tau_0^{1.006}. \quad (35)$$

For the range of disk parameters that are usually of interest, $\log\delta$ and $\log\tau_0$ have values between two and four. For these values, the considered combinations of $\Pi_1 - \Pi_4$ are essentially independent of radius, and a

single characteristic value may be used within each zone:

$$\text{zone B:}\quad \Pi_h \approx 2.6,\quad \Pi_\Sigma = 0.96,\quad \Pi_\rho = 0.67,\quad \Pi_\mathrm{T} = 1.2, \tag{36}$$

$$\text{zone C:}\quad \Pi_h \approx 2.6,\quad \Pi_\Sigma = 1.03,\quad \Pi_\rho = 0.76,\quad \Pi_\mathrm{T} = 1.09. \tag{37}$$

The boundary between zones B and C is roughly determined from the equality of κ_T and $\kappa_0\rho T^{7/2}$ in the plane of symmetry of the disk (for the characteristic values of the dimensionless parameters $\Pi_1 - \Pi_4$ and $f(R) = 1$):

$$R_\mathrm{BC} \sim 5\times 10^7 m^{1/3}\dot{M}_{17}^{2/3}\left(\frac{\mu}{0.6}\right)^{-1/3} \times \left(\frac{\kappa_0}{\kappa_0^*}\right)^{-2/3}\left(\frac{\kappa_\mathrm{T}}{\kappa_\mathrm{T}^*}\right)^{4/3}\ \mathrm{cm}.$$

We take the radius where recombination of hydrogen atoms begins (for $T_\mathrm{eff} \sim 10^4$ K) to be the outer boundary of zone C. In this case, the disk becomes unstable and convection begins to contribute to the energy transport towards the surface, due to the substantial increase in the opacity coefficient [4, 10]. In these regions, the opacity coefficient κ_r cannot be approximated by the Cramers law. We obtain from the condition $T_\mathrm{eff} = 10^4$ K, equating the right side of (15) and $\sigma_\mathrm{SB}T_\mathrm{eff}^4$:

$$R_\mathrm{C} \approx 1.4\times 10^{10} m^{1/3}\dot{M}_{17}^{1/3}\ \mathrm{cm}. \tag{38}$$

Let us consider a disk consisting purely of hydrogen plasma ($\mu = 0.5$), with the opacity $\kappa_\mathrm{r} = 6.4\times 10^{22}\rho T^{-7/2}\ \mathrm{cm}^2/\mathrm{g}$ [2] (a similar value was used in [1]), specified only by free–free transitions of electrons in the plasma. This is two orders of magnitude lower than the opacity for bound–free transitions κ_0^*, but the resulting variations of the physical quantities involved will be suppressed by the small power-law indices with which the opacity coefficient enters (27)–(30). For example, the disk half-thickness (27) will vary due to the decrease of κ_0 and μ, and also Π_h, since τ_0 will decrease by nearly a factor of 10 [see (32) and the lower graphs in Fig. 2]. We thus obtain for $\mu = 0.5$ a disk half-thickness h that is ~25% smaller than for $\mu = 0.62$.

If all the $\Pi_1 - \Pi_4$ values are unity in the formulas for the radial dependences of the physical parameters of the disk, $\kappa_\mathrm{T} = 0.4\ \mathrm{cm}^2/\mathrm{g}$, $\kappa_0 = 6.4\times 10^{22}\ \mathrm{cm}^5\ \mathrm{g}^{-2}\ \mathrm{K}^{7/2}$, and $\mu = 0.5$, these formulas coincide with the expressions for a standard α disk from [2, Sec. 3].

The numerical solution for the vertical structure equations yields a larger disk thickness than that for a uniform disk, or the so-called "characteristic hydrostatic size" v_s/ω, where v_s is the speed of sound in the plane of symmetry. The fact that the numerically calculated disk thickness is approximately twice the characteristic hydrostatic size was already noticed in [1, Fig. 11]. This increase is due to the inhomogeneity of the density and temperature distributions over the disk thickness, and corresponds to a factor of the order of $\sqrt{\Pi_1} \sim 2.5$ [15]:

$$h \cong \sqrt{\Pi_1}\sqrt{\frac{\mathcal{R}T_\mathrm{c}}{\mu}}\frac{1}{\omega}. \tag{39}$$

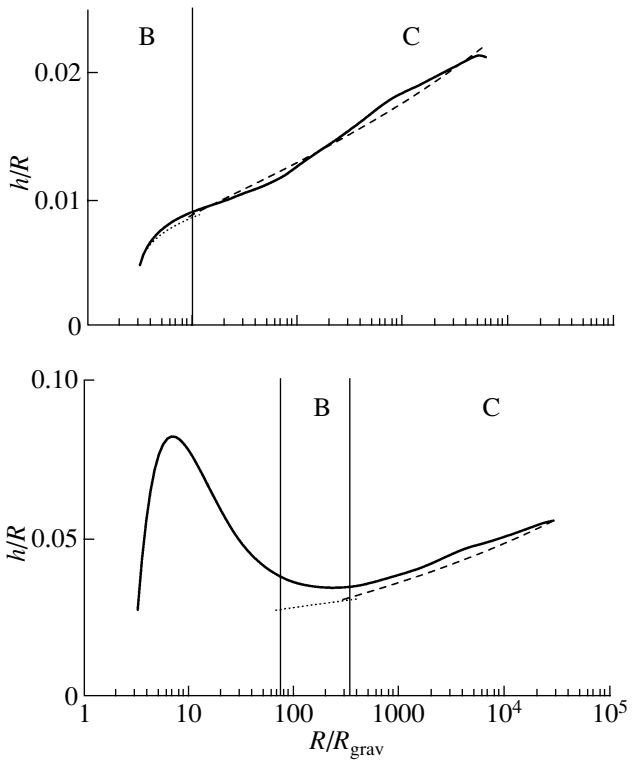

Fig. 3. Relative half-thickness of the disk. The disk parameters are $m = 10$, $R_\mathrm{grav} = 2GM/c^2 \approx 3\times 10^6$ cm, $\alpha = 0.3$, $\mu = 0.62$, and $\dot{M} = 3.36\times 10^{16}$ g/s (top) or $\dot{M} = 3.36\times 10^{18}$ g/s (bottom). The solid bold curve represents the exact model with the tabulated opacities and $P = P_\mathrm{rad} + P_\mathrm{gas}$; the dotted and dashed curves indicate the dependences for zones B and C, respectively, obtained using the analytical approximation for the opacity coefficient.

5. COMPARISON OF THE RESULTS OF THE VERTICAL STRUCTURE CALCULATIONS

We compare the results obtained using the two methods indicated above by plotting the radial dependences of the relative half-thickness, surface density,

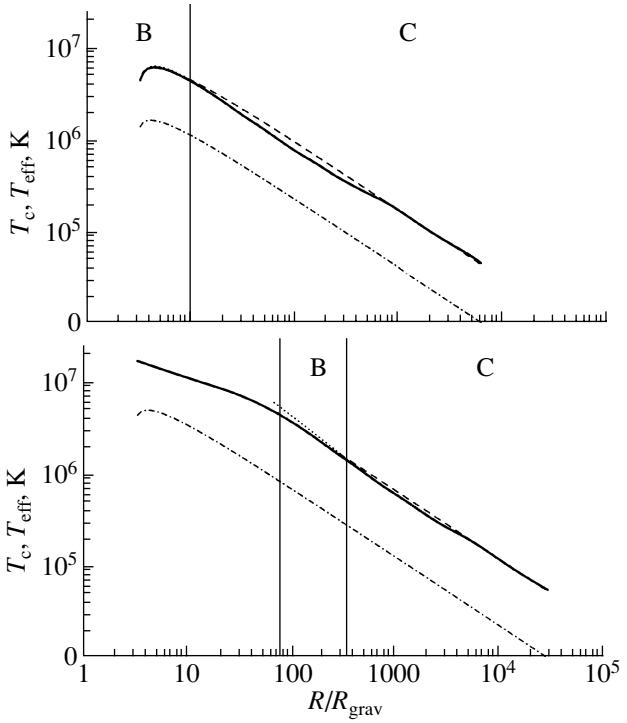

Fig. 4. Temperature in the plane of symmetry of the disk. The disk parameters and notation are the same as in Fig. 3. The dot–dashed curve shows the effective temperature $T_{\rm eff} = (Q_{\rm o}/\sigma_{\rm SB})^{1/4}$.

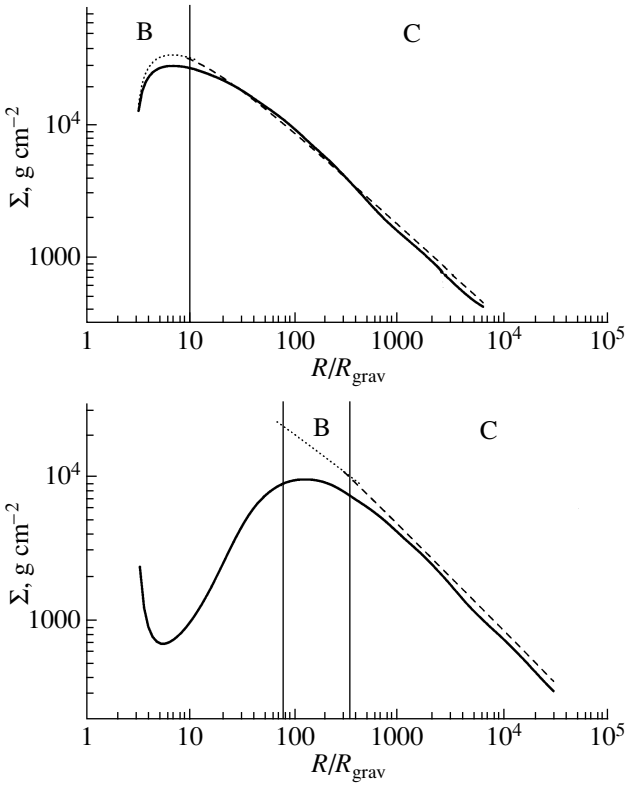

Fig. 5. Surface density of the disk. The disk parameters and notation are the same as in Fig. 3.

and density and temperature in the central plane of the disk. These dependences are constructed for two models of a accretion disk around a black hole with mass $M = 10\ M_\odot$, $\mu = 0.62$, $\alpha = 0.3$, and accretion rates corresponding to bolometric luminosities of the disk $0.002 L_{\rm Ed}$ and $0.2 L_{\rm Ed}$, where $L_{\rm Ed} = 1.26 \times 10^{39}$ erg/s is the Eddington luminosity for an object with mass $10\ M_\odot$. Figures 3–8 present the resulting dependences. The vertical lines indicate the formal boundaries between zones A, B, and C. Zone A is absent from the model on the upper graphs. The curves are shown out to the radius where the effective temperature is equal to 10^4 K.

The dotted curves indicate the dependences for zone B calculated from (18)–(21), and the dashed curves those for zone C calculated from (27)–(30). Except for Π_h, the dimensionless parameters are taken in accordance with (36) and (37). The parameter Π_h varies only slightly for variations in the accretion rate covering two orders of magnitude. We used $\Pi_h = 2.61$ in zone B and $\Pi_h = 2.58$ in zone C for $\dot{M} = 3.36 \times 10^{16}$ g/s, and $\Pi_h = 2.69$ in zone B and $\Pi_h = 2.67$ in zone C for $\dot{M} = 3.36 \times 10^{18}$ g/s.

The dependences expressed by the analytical formulas (dotted and dashed curves) closely correspond to the exact solution obtained for the tabulated opacities (bold solid curve) in regions where the radiation pressure is negligibly small. The disk half-thickness in zone C for $\dot{M} = 3.36 \times 10^{18}$ g/s calculated for the tabulated opacities differs from that obtained from (27), primarily due to the difference between the Cramers opacity law and the real (tabulated) opacities (lower graphs in Fig. 3). Recall that the relation $\kappa_0^* = 5 \times 10^{24}$ cm^5 g^{-2} K$^{7/2}$ will represent a more or less precise approximation, depending on the actual parameters of the accretion disk. Differences due to the contribution from the radiation pressure become appreciable when $P_{\rm rad}/P_{\rm gas} \gtrsim 0.2$–$0.3$.

The agreement between the results for the two numerical methods used to calculate the vertical structure of an accretion disk within their common region of applicability (where the role of radiation pressure can be neglected) also demonstrates the reliability of each of the methods, and justifies the use of (18)–(21) and (27)–(30) to describe the radial structure of the disk in zones B and C between the radii estimated by (26) and (38), provided that the radiation pressure in zone B does not exceed $0.3\ P_{\rm gas}$.

6. DISCUSSION OF THE RESULTS

The half-thickness of the outer parts of a classical, optically thick α accretion disk with solar chemical

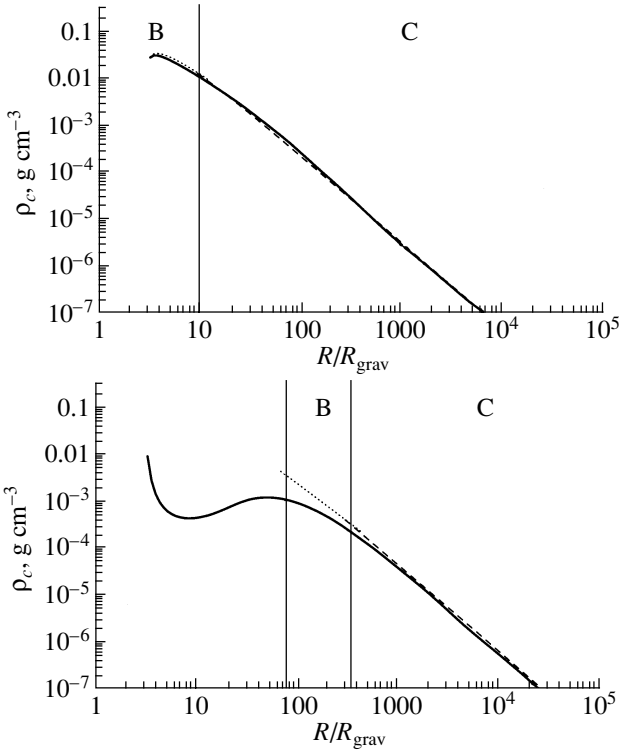

Fig. 6. Density in the plane of symmetry of the disk. The disk parameters and notation are the same as in Fig. 3.

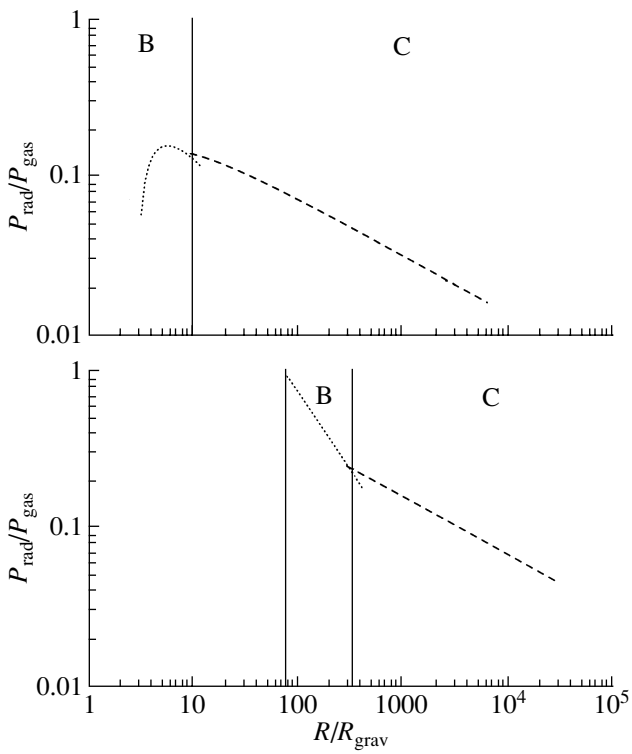

Fig. 7. Radio of the radiation and gas pressures in the plane of symmetry of the disk. The disk parameters and notation are the same as in Fig. 3.

composition in the zone of total ionization of hydrogen is [see (27) and (37)]:

$$\frac{h_{\rm d}}{R} = 0.05 m^{-3/8} \dot{M}_{17}^{3/20} \alpha^{-1/10} R_{10}^{1/8}.$$

As noted above, this formula is valid in zones where the energy is transported to the surface by radiation. In regions more distant from the center, where hydrogen recombination begins and convection develops, the disk thickness decreases, and its surface appears to be in shadow [10]. Therefore, we will restrict our consideration to a disk with fully ionized hydrogen and $T_{\rm eff} \gtrsim 10^4$ K. We will also assume that the maximum relative disk half-thickness $h_{\rm d}/R$ is reached at the radius where $T_{\rm eff} = 10^4$ K.

We can then write an expression for the maximum relative disk half-thickness as a function of the disk parameters:

$$\frac{h_{\rm d}}{R}(\max) = 0.093 m^{-17/120} \alpha^{-1/10} \dot{m}^{23/120}, \quad (40)$$

where $\dot{m}$ is the accretion rate normalized to the critical value $1.26 \times 10^{38}(m/\eta c^2)$ corresponding to the Eddington bolometric luminosity. We adopt the value $\eta = 1/12$. It follows readily from this expression that $h_{\rm d}/R \approx 0.1$ for $\alpha = 0.1$ for high-luminosity disks ($\dot{m} \approx 1$) around neutron stars in low-mass X-ray binaries. Disks around black holes with masses $\sim 10\, M_\odot$ in X-ray novae at their maximum brightness ($\dot{m} \sim 0.5$) and with the same value of α theoretically have maximum relative half-thicknesses ~ 0.07. Consequently, the relative half-thicknesses of α disks cannot substantially exceed 0.1. Recall that we are considering disks with accretion rates below the critical value: $\dot{m} \lesssim 1$.

Let us compare the obtained value with the observations. Data for 11 fairly well studied X-ray novae with black holes [30] indicate an absence of systems whose orbital planes are inclined to the line of sight by more than 75°. The scarcity of eclipses in X-ray novae with black holes and neutron stars also leads to the conclusion that they are not observed "edge-on" [30, 31]. It is concluded in these studies that, in these systems, the X-ray radiation from the inner plane of the disk is blocked by some parts of the disk or structures above it (such as the disk chromosphere or corona) that posses appreciable relative thicknesses of the order of or exceeding the tangent of the half-angle at which the secondary component is seen from the compact object: $\sim 0.15-0.25$. The same pattern of matter distribution in the form of a corona above the disk follows from analyses of the X-ray light curves of relatively rare eclipsing X-ray binaries [32, 33]. The broad (about a third of the orbital period)

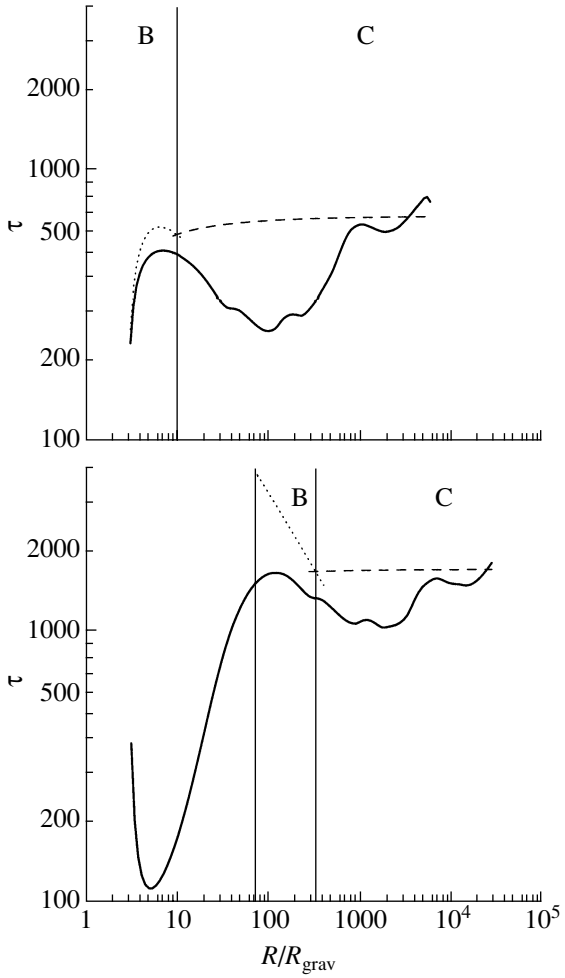

Fig. 8. Optical depth of the disk. The disk parameters and notation are the same as in Fig. 3. The dotted curve in zone B is calculated from (23), and the dashed curve in zone C from (35).

minima provide evidence that we see very extended sources of X-ray radiation in these systems. This is most likely radiation scattered in the corona above the disk, whereas the primary X-ray source (inner parts of the disk and the central source, if there is one) is not visible.

Some information about the geometry of re-emitting regions can also be derived via reverberation mapping (see, for example, [34, 35]), which is based on analyzing the delays between variations of the X-ray and optical fluxes, which depend on the distances covered by the X-ray photons between their emission and re-emission. O'Brien et al. [34] obtained a relative disk half-thickness at the outer radius $\sim$0.24 for the low-mass X-ray binary GRO J1655−40. The increased relative thickness of the outer parts of accretion disks also follows from the large ratio of the optical and X-ray fluxes for the same X-ray novae during flares [36, 37], and also for super-soft X-ray sources [38, 39]. The same result is provided by analyses of the optical variability amplitude of low-mass X-ray binaries due to the reflection of radiation from the disk and secondary component [40]. Such estimates are based on the fact that an appreciable fraction of the optical disk radiation is due to the reprocessing of hard X-ray radiation, which depends on the geometry of the regions intercepting the radiation and the nature of the central source.

Gilfanov and Arefiev [41] suggest a technique for estimating the largest "viscous" time scales in accretion disks using the position of the break in the power spectra of the X-ray variations in low-mass X-ray binaries. This time scale can then be used to derive the half-thickness at the outer edge of the disk, which turns out to substantially exceed the standard disk thickness. Based on an analysis of the power spectra of 12 objects, Gilfanov and Arefiev [41] concluded that a substantial part of the accretion flux can be described by an optically thin hot "coronal flux" with a characteristic size of $h/R \gtrsim 0.1$–0.3. However, the time variability of disks is complex, and requires further studies.

Let us analyze possible ways to increase the thickness of an α disk and bring the theory and observations into agreement.

Essentially, to increase the model disk thickness, it is sufficient to increase the temperature in the plane of symmetry [see (39)]. However, this will be accompanied by a dramatic decrease in the opacity, and, accordingly, in the optical depth of the disk. There is a "brightening" of the disk, leading to a decrease in Π_1, so that the half-thickness of the disk remains virtually constant [see also (39)].

On the other hand, we can increase the surface density of the disk Σ. In this case, its optical depth and the temperature in the central plane will also increase, since $T_{\rm c} \sim (\kappa_{\rm r}\Sigma)^{1/4} T_{\rm eff}$. Simple estimates show that the disk luminosity can only be maintained by a decrease in the disk viscosity by many orders of magnitude, i.e., by an α value of the order of 10^{-6}. Such values of α seem unlikely, since the dynamics of the fading of dwarf [5, 6] and X-ray novae [7, 8, 37, 42] can be explained well by models with a geometrically thin, non-stationary accretion disk with $\alpha \sim 0.1$–1 for zones with total ionization.

Another hypothetical way to increase the temperature in the central plane of the disk is illumination of the outer disk by hard radiation. The ratio of the flux illuminating a disk surface element located at the angle $\approx ({\rm d}h_{\rm irr}/{\rm d}R - h_{\rm irr}/R)$ and the internal flux due

to viscous friction (see, for example, [1, 43], and also (15)) is

$$\frac{Q_{\rm irr}}{Q_0} = \frac{4}{3}\eta\Psi(\theta)(1-A_{\rm x}) \times \frac{h_{\rm irr}}{R}\left(\frac{{\rm d}\ln h_{\rm irr}}{{\rm d}\ln R}-1\right)\frac{R}{R_{\rm grav}} \equiv \frac{4}{3}\eta\mathcal{C}\frac{R}{R_{\rm grav}}, \quad (41)$$

where $h_{\rm irr}$ is the height at which the X-ray radiation is intercepted, $\eta \sim 0.1$ the accretion efficiency, $1-A_{\rm x}$ the fraction of incoming flux that is subject to thermalization, which depends on the disk albedo and the spectral energy distribution of the central source [44], and $R_{\rm grav} = 2GM/c^2$. For the standard disk profile, the expression in brackets on the second line of formula (41) is equal to 1/8 [see (27)].

The function $\Psi(\theta)$ describes the angular distribution of the central radiation: the flux depends on the angle as $\Psi(\theta)L/4\pi R^2$, where θ is the angle between the normal to the plane of the central part of the disk and the direction from the central disk towards the illuminated disk surface element. In the case of a point-like central source, $\Psi(\theta) = 1$; for a flat central disk, $\Psi(\theta) = 2\cos(\theta)$ [45, 46]. The second case may become realistic if the central object is a black hole. Then, for large θ, the approximation $\cos\theta \approx h_{\rm irr}/R$ is commonly used, valid for geometrically thin outer disks.

The temperature in the plane of symmetry of the disk can be estimated as

$$T_{\rm c}^4 \cong \frac{3}{8}\tau_0 T_{\rm eff}^4 + T_{\rm irr}^4,$$

where $T_{\rm irr}^4 = Q_{\rm irr}/\sigma_{\rm SB}$. For example, to double the disk thickness, the temperature must be increased by a factor of four, which requires that the flux exceed the intrinsic flux by a factor of $\sim 95\tau_0$, since

$$\frac{Q_{\rm irr}}{Qo} \cong \frac{3\tau_0}{8}\left(\left(\frac{T_c^{new}}{T_c^{old}}\right)^4 - 1\right).$$

According to (33), for $\alpha = 0.5$, $\tau_0 \sim 1000$ for a disk with solar chemical composition and $\tau_0 \sim 170$ for a pure hydrogen disk. We can obtain an upper estimate for the flux ratio from (41):

$$\frac{Q_{\rm irr}}{Q_0} \approx 75\frac{\mathcal{C}}{5\times 10^{-3}}\left(\frac{\eta}{0.1}\right)^{2/3}\frac{\dot{m}^{1/3}}{m^{1/3}}.$$

This estimate is obtained for the outer boundary of zone C [see (38)]. Thus, this formal analysis likewise does not yield illumination sufficient to make the disk appreciably thicker for any chemical composition.

Moreover, based on their calculations of the vertical structure of the illuminated disk, Meshcheryakov et al. [23] argue that, in the case of deep heating of a stationary disk by an external flux, the temperature in the central plane of the disk increases, the surface density and optical depth decrease, and the geometrical thickness remains essentially constant.

In a number of studies, disk thicknesses are determined from the ratio of the X-ray and optical fluxes; these studies essentially determine the illumination parameter. Let us consider this in more detail:

$$\mathcal{C} = \Psi(\theta)(1-A_{\rm x})\frac{h_{\rm irr}}{R}\left(\frac{{\rm d}\ln h_{\rm irr}}{{\rm d}\ln R}-1\right),$$

which we normalized above to the characteristic value (see, for example, [7] and references therein). $\mathcal{C}$ can be determined from the observed X-ray-to-optical flux ratio, and combines the relatively poorly known thickness and albedo of the disk. Therefore, it is convenient to use this quantity for comparison with the predictions of different models.

It is important that taking into account general-relativistic effects on the propagation of light near a black hole increases $\Psi(\theta)$ in comparison with the case of a flat metric for larger θ. The trajectories of photons are concentrated towards the disk plane, mainly due to aberration [47]. For example, for a flat disk around a rapidly rotating Kerr black hole with $a_{\rm Kerr} = 0.9981$, the factor $\Psi(\theta)$ in the direction $\cos\theta \sim 0.1$ exceeds that for light propagation in a flat space by a factor of three to four (Fig. 9). Taking into account limb darkening of the radiation emitted from the disk surface results in a decrease in the number of photons at larger θ. The coefficient in the limb darkening law is $u = 0$ for a local isotropic propagation of photons from the disk surface, $u = 1.5$ for a gray atmosphere, and $u = 2.06$ for an atmosphere dominated by electron scattering [48, 49]. In Fig. 9, the dashed curve indicates the dependence $\Psi(\theta)$ taking into account the re-processing of photons that have returned to the disk.

In a first approximation, let us assume that the disk profile corresponds to the standard model. Then, without taking into account the relativistic amplification, we obtain for a flat disk

$$\mathcal{C} \sim 6\times 10^{-5}\left(\frac{h_{\rm irr}/R}{0.05}\right)^2\frac{1-A_{\rm x}}{0.1} \quad (42)$$

and for a point source

$$\mathcal{C} \sim 6\times 10^{-4}\left(\frac{h_{\rm irr}/R}{0.05}\right)\frac{1-A_{\rm x}}{0.1}.$$

If an isotropically radiating source is located at a height $Z_{\rm x}$ above the plane of symmetry, $\mathcal{C}$ will increase by a factor of $1 + (Z_{\rm x}/h_{\rm irr})({\rm d}\ln h_{\rm irr}/{\rm d}\ln R - 1)^{-1}$ [50].

In their modelling of X-ray and optical light curves, Esin et al. [36] found that, $\mathcal{C} \sim 0.004$ for the X-ray nova A 0620-00 (1975) at the epoch when the central X-ray source was a disk, and $\mathcal{C} \sim 0.0014$ for

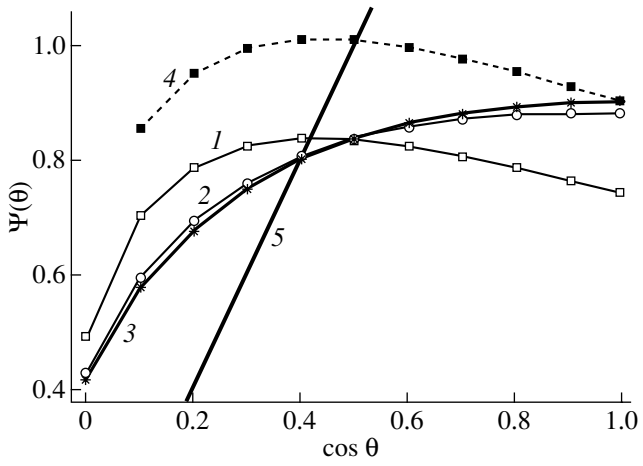

Fig. 9. Angular distribution of the disk radiation, taking into account general-relativistic effects. Curves *1–3* are calculated using the code from [68] for the coefficients in the limb darkening law $u = 0$, 1.5 and 2.6, respectively. Curve *4* is calculated for $u = 0$ and takes into account the re-processing of photons returning to the disk in the model *kerrbb* from the XSPEC 11.3.1 package [69], using the code described in [70]. The straight line *5* displays the function $\Psi(\theta) = 2\cos\theta$ for a Newtonian metric.

GS 1124-683 (1991). For an outburst of A 0620-00 about 10–50 days after the peak, the model of [37] yields $\mathcal{C} \sim (6–9) \times 10^{-3}$. On the other hand, $\mathcal{C} \sim 0.002–0.004$ was found for low-mass X-ray binaries with neutron stars in [40].

Thus, according to (42) for the efficiency of reprocessing of X-ray radiation $1 - A_x \sim 0.1$ [44], the maximum thickness for a standard disk $h_{irr}/R \sim 0.05–0.1$, and including a relativistic amplification $\sim$4, we obtain $\mathcal{C} \sim 0.00025–0.001$. It follows that, generally speaking, either the disk thickness must exceed the standard value, or the efficiency of the reprocessing of the X-ray radiation 0.1 is too low to fit the observations, or both these values must be increased over their standard values. A similar conclusion is obtained for the case of a central point source.

If the disk has a hot corona, the main process in this corona will be the scattering of hard photons on free electrons; further, these photons can penetrate into sub-photospheric layers of the disk, where they can be absorbed [23, 51]. As a result of the interception of X-rays in the corona, the effective half-thickness of the disk with regards to this process h_{irr} turns out to exceed the standard value h_d by a factor of 1.5–2.5. Models for the corona were considered in [51–57]. The matter above the disk can also form a layer of gas flowing from the companion (see, for example, [58–60]).

Due to thermal instability, a two-phase medium may appear above a standard disk, consisting of clouds with temperatures $\sim 10^4$ K and inter-cloud material with a temperature about two orders of magnitude higher. A model with multiple scattering of X-rays on the clouds is suggested in [61], and the resulting factor for the reprocessing of X-rays into optical radiation $1 - A_x$ increases to 0.3–0.5.

We can also consider a warped disk that can intercept a substantial fraction of the central radiation. It was suggested in [14, 36] that the disks in low-mass X-ray binaries may be twisted, as in Her X-1 [62]. Disk could be bent due to a number of effects, such as the Lenz–Thirring effect [63], radiation pressure [64, 65], etc.

Calculations of $\mathcal{C}$ carried out in [66] for a disk warped by torques due to radiation pressure show that this quantity can be appreciable, even for the case of a high disk albedo (for an isotropically radiating central source). On the other hand, it was concluded that only a small number of low-mass X-ray binaries (primarily those with long periods) can develop such disk warping.

When the disk is warped because the rotational angular momentum of the black hole and the orbital angular momentum of the binary have different directions, the disk geometry depends on the ratio of the viscous parameter α and the disk half-thickness (see, for example, [67]). Such a disk can be represented roughly as having two parts: an outer region in the orbit plane of the binary, and a twisted inner region. Suppose that the intrinsic disk half-thickness is insignificant (as for a standard disk). If the central source radiates isotropically, the interception of the X-ray flux by such a disk does not increase. However, in the case of anisotropic radiation (which is quite expected, since the central object is a black hole), we will likewise not obtain an appreciable increase in the fraction of intercepted flux. When we take into account general-relativistic effects on the propagation of photons, the directional pattern of the radiation of a

flat disk becomes more isotropic (Fig. 9). In addition, the area of the illuminated surface is a factor of two smaller for a warped disk. For example, if the relative disk half-thickness is ~ 0.05, the disk will intercept a flux $L_x(0.05)^2/r^2$ for $\Psi(\theta) = 2\cos\theta$ when it lies completely in a plane. Applying the angular distribution for a black hole with the maximum angular momentum and including limb darkening with a factor of 1.5 (circles in Fig. 9), we find that, in fact, an unwarped disk intercepts a flux equal to $\sim 0.024 L_x/r^2$, i.e., larger by an order of magnitude. Suppose that the outer parts of such a disk are inclined so that the tangent of the angle between the plane of the disk and the equatorial plane of the black hole is $0.2R$; a simple calculation yields that half the disk intercepts only $\sim 0.015 L_x/r^2$.

It thus seems more likely that the observed half-thicknesses of accretion disks are due to the presence of matter above their surfaces (in the form of a corona and/or wind) that is optically thick in the radial direction. Under some conditions, this medium may be inhomogeneous.

7. CONCLUSION

We have described a method for calculating the vertical structure of a standard α disk. Based on an independent method for calculating this structure [15], we obtained analytical radial dependences for the disk parameters, which yield an explicit dependence on the opacity coefficient. We have demonstrated the consistency of the two methods in the region where the model assumptions are the same, i.e., where hydrogen is fully ionized and the radiation pressure can be neglected.

The numerical solution for the equations describing the vertical structure of the disk with a standard elemental abundance yields a thickness that is nearly a factor of three larger than the so-called "characteristic hydrostatic size." Such a disk is thicker than a pure hydrogen disk by about 25%.

We discussed the discrepancy between the observed characteristics of binary systems with accretion disks and theoretical predictions for the disk thickness. To bring the standard disk model into agreement with the observations, matter above the disk that intercepts the X-ray radiation must be taken into consideration. In the presence of a hot corona above the disk that scatters X-ray radiation, the thickness h_{irr} with regards to this process can exceed the thickness of a standard disk h_d by a factor of 1.5–3. In this case, both the the statistics of eclipses in binaries and the optical flux from the accretion disks in X-ray sources can be explained.

ACKNOWLEDGMENTS

The study was supported by the Russian Foundation for Basic Research (project nos. 06-02-16025-a and 05-02-17744) and the Program of Support for Leading Scientific Schools of the Russian Federation (grant NSh-784.2006.2). G.V. Lipunova thanks Y.Y. Kovalev for his support. N.I. Shakura is grateful to the Max Planck Institute for Astrophysics (Garching, Germany) for providing him with the opportunity for annual short-term visits for studies.

REFERENCES

1. N. I. Shakura and R. A. Sunyaev, Astron. Astrophys. **24**, 337 (1973).
2. S. Kato, J. Fukue, and S. Mineshige, *Black-Hole Accretion Disks* (Kyoto Univ. Press, Kyoto, Japan, 1998).
3. J. Frank, A. King, and D. J. Raine, *Accretion Power in Astrophysics* (Cambridge Univ. Press, Cambridge, UK, 2002).
4. F. Meyer and E. Meyer-Hofmeister, Astron. Astrophys. **104**, L10 (1981).
5. J. Smak, Acta Astron. **34**, 161 (1984).
6. J. K. Cannizzo, *Accretion Disks in Compact Stellar Systems* (1993), p. 6.
7. G. Dubus, J.-M. Hameury, and J.-P. Lasota, Astron. Astrophys. **373**, 251 (2001).
8. G. V. Lipunova and N. I. Shakura, Astron. Astrophys. **356**, 363 (2000).
9. G. V. Lipunova and N. I. Shakura, Astron. Zh. **79**, 407 (2002) [Astron. Rep. **46**, 366 (2002)].
10. F. Meyer and E. Meyer-Hofmeister, Astron. Astrophys. **106**, 34 (1982).
11. G. Shaviv and R. Wehrse, Astron. Astrophys. **159**, L5 (1986).
12. V. F. Suleĭmanov, Pis'ma Astron. Zh. **18**, 255 (1992) [Sov. Astron. Lett. **18**, 104 (1992)].
13. J.-M. Hameury, K. Menou, G. Dubus, et al., Mon. Not. R. Astron. Soc. **298**, 1048 (1998).
14. G. Dubus, J.-P. Lasota, J.-M. Hameury, and P. Charles, Mon. Not. R. Astron. Soc. **303**, 139 (1999).
15. N. A. Ketsaris and N. I. Shakura, Astron. Astrophys. Trans. **15**, 193 (1998).
16. J. K. Cannizzo, Astrophys. J. **385**, 94 (1992).
17. R. L. Kurucz, *Atlas: A Computer Program for Calculating Model Stellar Etmospheres,* SAO Special Report (Smithsonian Astrophys. Obs., Cambridge, 1970).
18. R. Kurucz, *Kurucz CD-ROMs* (Smithsonian Astrophys. Obs., Cambridge, 1993).
19. V. F. Suleĭmanov, Pis'ma Astron. Zh. **17**, 575 (1991) [Sov. Astron. Lett. **17**, 245 (1991)].
20. A. P. Lightman and D. M. Eardley, Astrophys. J. **187**, L1 (1974).
21. N. Shibazaki and R. Hōshi, Progr. Theor. Phys. **54**, 706 (1975).
22. N. I. Shakura and R. A. Sunyaev, Mon. Not. R. Astron. Soc. **175**, 613 (1976).

23. A. V. Mescheryakov, R. A. Likhachev, and N. I. Shakura, Astron. Zh. (2007) (in preparation).
24. N. I. Shakura, Astron. Zh. **49**, 921 (1972) [Sov. Astron. **16**, 756 (1973)].
25. R. J. Tayler, Mon. Not. R. Astron. Soc. **191**, 135 (1980).
26. N. Grevesse and E. Anders, in *Cosmic Abundances of Matter*, Ed. by C. J. Waddington (Am. Inst. Phys., 1989), AIP Conf. Proc. **183**, 1.
27. Yu. É. Lyubarskiĭ and N. I. Shakura, Pis'ma Astron. Zh. **13**, 917 (1987) [Sov. Astron. Lett. **13**, 386 (1987)].
28. Ya. B. Zel'dovich and N. I. Shakura, Astron. Zh. **46**, 225 (1969) [Sov. Astron. **13**, 175 (1969)].
29. D. Mihalas, *Stellar Atmospheres* (Freeman, San Francisco, 1978; Mir, Moscow, 1982).
30. R. Narayan and J. E. McClintock, Astrophys. J. **623**, 1017 (2005).
31. M. Milgrom, Astron. Astrophys. **67**, L25 (1978).
32. J. E. McClintock, R. A. London, H. E. Bond, and A. D. Grauer, Astrophys. J. **258**, 245 (1982).
33. Z. Ioannou, T. Naylor, A. P. Smale, P. A. Charles, and K. Mukai, Astron. Astrophys. **382**, 130 (2002).
34. K. O'Brien, K. Horne, R. I. Hynes, et al., Mon. Not. R. Astron. Soc. **334**, 426 (2002).
35. R. I. Hynes, in *The Astrophysics of Cataclysmic Variables and Related Objects*, Ed. by J.-M. Hameury and J.-P. Lasota (Astron. Soc. Pac., San Francisco, 2005a), Astron. Soc. Pac. Conf. Ser. **330**, 237.
36. A. A. Esin, E. Kuulkers, J. E. McClintock, and R. Narayan, Astrophys. J. **532**, 1069 (2000).
37. V. F. Suleimanov, G. V. Lipunova, and N. I. Shakura, in *Proceedings of the 5th INTEGRAL Workshop on the INTEGRAL Universe*, Ed. by V. Schoenfelder, G. Lichti, and C. Winkler (European Space Agency, 2004), ESA SP-552, p. 403.
38. R. Popham and R. Di Stefano, *Accretion Disks in Supersoft X-ray Sources*, Tech. Rep. Smithson. Astrophys. Obs. (Smithson. Astrophys. Obs., Cambridge, 1996).
39. S. Schandl, E. Meyer-Hofmeister, and F. Meyer, Astron. Astrophys. **318**, 73 (1997).
40. J. A. de Jong, J. van Paradijs, and T. Augusteijn, Astron. Astrophys. **314**, 484 (1996).
41. M. Gilfanov and V. Arefiev, astro-ph/0501215 (2005).
42. Ü. Ertan and M. A. Alpar, Astron. Astrophys. **393**, 205 (2002).
43. A. R. King and H. Ritter, Mon. Not. R. Astron. Soc. **293**, L42 (1998).
44. V. Suleimanov, F. Meyer, and E. Meyer-Hofmeister, Astron. Astrophys. **350**, 63 (1999).
45. N. G. Bochkarev, R. A. Syunyaev, T. S. Khruzina, et al., Astron. Zh. **65**, 778 (1988) [Sov. Astron. **32**, 405 (1988)].
46. J. Fukue, Publ. Aston. Soc. Jpn. **44**, 663 (1992).
47. C. T. Cunningham, Astrophys. J. **202**, 788 (1975).
48. S. Chandrasekhar, *Radiative Transfer* (Dover, New York, 1960; Inostrannaya Literatura, Moscow, 1953).
49. A. Laor, H. Netzer, and T. Piran, Mon. Not. R. Astron. Soc. **242**, 560 (1990).
50. R. I. Hynes, Astrophys. J. **623**, 1026 (2005b).
51. M. A. Jimenez-Garate, J. C. Raymond, and D. A. Liedahl, Astrophys. J. **581**, 1297 (2002).
52. M. C. Begelman and C. F. McKee, Astrophys. J. **271**, 89 (1983).
53. M. de Kool and D. Wickramasinghe, Mon. Not. R. Astron. Soc. **307**, 449 (1999).
54. A. Różańska and B. Czerny, Astron. Astrophys. **360**, 1170 (2000).
55. F. Meyer, B. F. Liu, and E. Meyer-Hofmeister, Astron. Astrophys. **361**, 175 (2000).
56. K. A. Miller and J. M. Stone, Astrophys. J. **534**, 398 (2000).
57. J. M. Miller, J. Raymond, A. Fabian, et al., Nature **441**, 953 (2006).
58. J. Frank, A. R. King, and J.-P. Lasota, Astron. Astrophys. **178**, 137 (1987).
59. P. J. Armitage and M. Livio, Astrophys. J. **470**, 1024 (1996).
60. D. V. Bisikalo, P. V. Kaĭgorodov, A. A. Boyarchuk, and O. A. Kuznetsov, Astron. Rep. **49**, 701 (2005).
61. V. Suleimanov, F. Meyer, and E. Meyer-Hofmeister, Astron. Astrophys. **401**, 1009 (2003).
62. N. I. Shakura, N. A. Ketsaris, M. E. Prokhorov, and K. A. Postnov, Mon. Not. R. Astron. Soc. **300**, 992 (1998).
63. J. M. Bardeen and J. A. Petterson, Astrophys. J. **195**, L65 (1975).
64. J. A. Petterson, Astrophys. J. **216**, 827 (1977).
65. J. E. Pringle, Mon. Not. R. Astron. Soc. **281**, 357 (1996).
66. G. I. Ogilvie and G. Dubus, Mon. Not. R. Astron. Soc. **320**, 485 (2001).
67. S. H. Lubow, G. I. Ogilvie, and J. E. Pringle, Mon. Not. R. Astron. Soc. **337**, 706 (2002).
68. R. Speith, H. Riffert, and H. Ruder, Comput. Phys. Commun. **88**, 109 (1995).
69. K. A. Arnaud, in: *Astronomical Data Analysis Software and Systems V*, Ed. by G. H. Jacoby and J. Barnes (Astron. Soc. Pac., San Francisco, 1996), Astron. Soc. Pac. Conf. Ser. **101**, 17.
70. L.-X. Li, E. R. Zimmerman, R. Narayan, and J. E. McClintock, Astrophys. J., Suppl. Ser. **157**, 335 (2005).

Translated by K. Maslennikov